Supporting Information

Magneli-Type Tungsten Oxide Nanorods as Catalysts for the Selective Oxidation of Organic Sulfides

René Dören[a], Jens Hartmann[a], Benjamin Leibauer, Martin Panthöfer, Mihail Mondeshki, and Wolfgang Tremel*

[a] These authors contributed equally to this work.

Department Chemie, Johannes Gutenberg-Universität Mainz, Duesbergweg 10-14, D-55128 Mainz, Germany

Table of Contents

Materials. All chemicals were used as received without further purification. Choline chloride (≥ 98 %) and cerium(III) nitrate hexahydrate (99.5 %, REacton) was purchased from Alfa Aesar, urea (99.5 %, analytical grade) was bought from Acros organics.

Tungsten oxide nanoparticle synthesis. WO_{3-x} nanorods (conditions **NR-1**) and ammonium tungsten bronze ($(NH_4)_{\sim 0.2}WO_3$) nanoparticles (conditions **ATB-15c**) were synthesized according to our previous publication.[1]

CeO_2 nanoparticle synthesis. CeO_2 nanoparticles were synthesized based on a synthesis of Hammond et. al.[2] Choline chloride and urea were mixed in molar ratio of 2:1 and heated to 80 °C for 14 h to gain the deep eutectic solvent reline. The reline was dried at 70 °C under reduced pressure for 6 h. $Ce(NO_3)_3 \cdot 6H_2O$ (750 mg; 1.7 mmol) was dissolved in reline (40 mL), transferred into a stainless steel autoclave (total volume: 50 mL) and heated to 100 °C for 10 h. The highly viscous gel-like reaction mixture was poured into Milli-Q-water (140 mL). The purple product was separated from the suspension by centrifugation (6000-9000 rpm, 10 min), washed three times with Milli-Q-water and three times with ethanol and dried at 80 °C for 14 h. The nanoparticles were calcined at 300 °C for 5 h bevor being used in catalytic experiments.

TiO_2 nanoparticles. Anatase TiO_2 nanoparticles were synthesized according our previous study,[3] based on a synthesis published by Dinh et. al.[4]

General Considerations. We attribute slight variations for the different standard *in situ* reactions mainly to residual moisture in the different methanol-d_4 batches, water adsorbed to the particles from air, as well as small weighing/pipetting errors.

Table S1. Product composition with additional water to standard *in situ* experiment (0.85 mg WO_{3-x} nanorods, 0.04 mmol thioanisole, 0.06 mmol H_2O_2 (60%) in 0.6 ml methanol-d_4).

Addition of water / µl	Ratio sulfide:sulfoxide:sulfone (10 min)	Ratio sulfide:sulfoxide:sulfone (30 min)
0	39:60:1	8:91:2
2.34[a]	50:50:0	14:85:1
2.34[b]	48:52:0	12:87:1
10[a]	73:26:1	36:62:2
10[b]	75:25:0	39:61:0
50[a,c]	92:8:0	72:28:0
50[b,c]	92:8:0	74:26:0
200[a,c]	92:7:1	79:21:0
200[b,c]	93:7:0	79:21:0

a. addition of H_2O. b. addition of D_2O. c. total volume fixed to 600 µl.

$$r = a * e^{-b*V} + c$$

r = conversion / %

V= added volume of H_2O / D_2O

Table S2. Fit parameters for water curves according to the equation above.

Curve	a	b	c
D_2O 10 min	55.059	0.108	7.256
H_2O 10 min	53.252	0.100	7.775
D_2O 30 min	72.944	0.057	21.365
H_2O 30 min	71.523	0.051	21.457

Table S3. Product composition after annealing at different temperatures for standard *in situ* experiment (0.85 mg WO_{3-x} nanorods, 0.04 mmol thioanisole, 0.06 mmol H_2O_2 (60%) in 0.6 ml methanol-d_4).

Annealing temperature / °C	Crystallographic phase	Ratio sulfide:sulfoxide:sulfone (10 min)	Ratio sulfide:sulfoxide:sulfone (30 min)
70[a]	WO_{3-x}	96:4:0	90:10:0
200	WO_{3-x}	92:8:0	88:12:0
250	WO_{3-x}	51:49:0	17:82:1
300	WO_{3-x}	39:60:1	8:90:2
350	WO_{3-x}	70:30:0	41:58:0
400	WO_{3-x}	77:23:0	55:45:0
500	WO_3 (monoclinic)	97:3:0	97:3:0

a. Particles additionally dried @ 40 °C under reduced preasure (~$1*10^{-2}$ mbar), 1.7 mg particles in 0.6 ml methanol-d_4, 0.2 mmol thioanisole, 0.3 mmol H_2O_2 (60 %).

Table S4. BET surface area and ζ – potential of nanoparticles used for sulfide oxidation.

catalyst	Specific surface area / m^2g^{-1}	ζ – potential / mV
WO_{3-x} nanorods	47.0	-39.7
$(NH_4)_{0.2}WO_3$ nanoparticles	22.8	-36.8
WO_3 reference (monoclinic)	2.7	-39.3
CeO_2 nanoparticles	133.9	23.8
TiO_2 nanoparticles	151.7	-9.1
TiO_2 P25	49.7	17.7

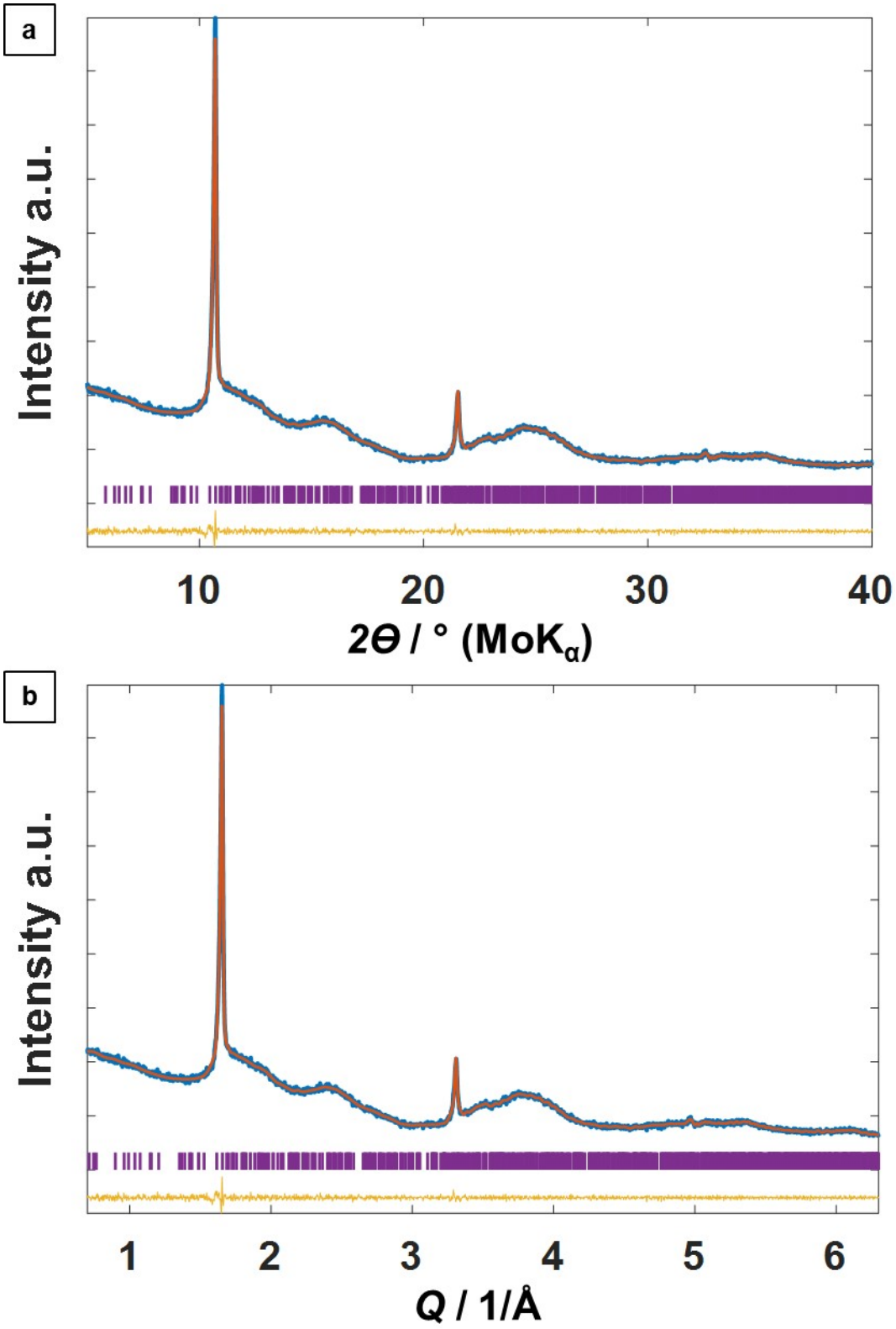

Fig. S1. Pawley refinements of WO_{3-x} NRs annealed at 300°C using space group *P2/m* and a quadratic form to compensate the anisotropy.[1] Refined parameters are: R_{wp}: 2.23, GOF: 1.08, crystal size (a*b*c): 4.1*72.6*4.3 nm. Lattice parameters: *a*=18.196 Å, *b*=3.794 Å and *c*= 14.000 Å.

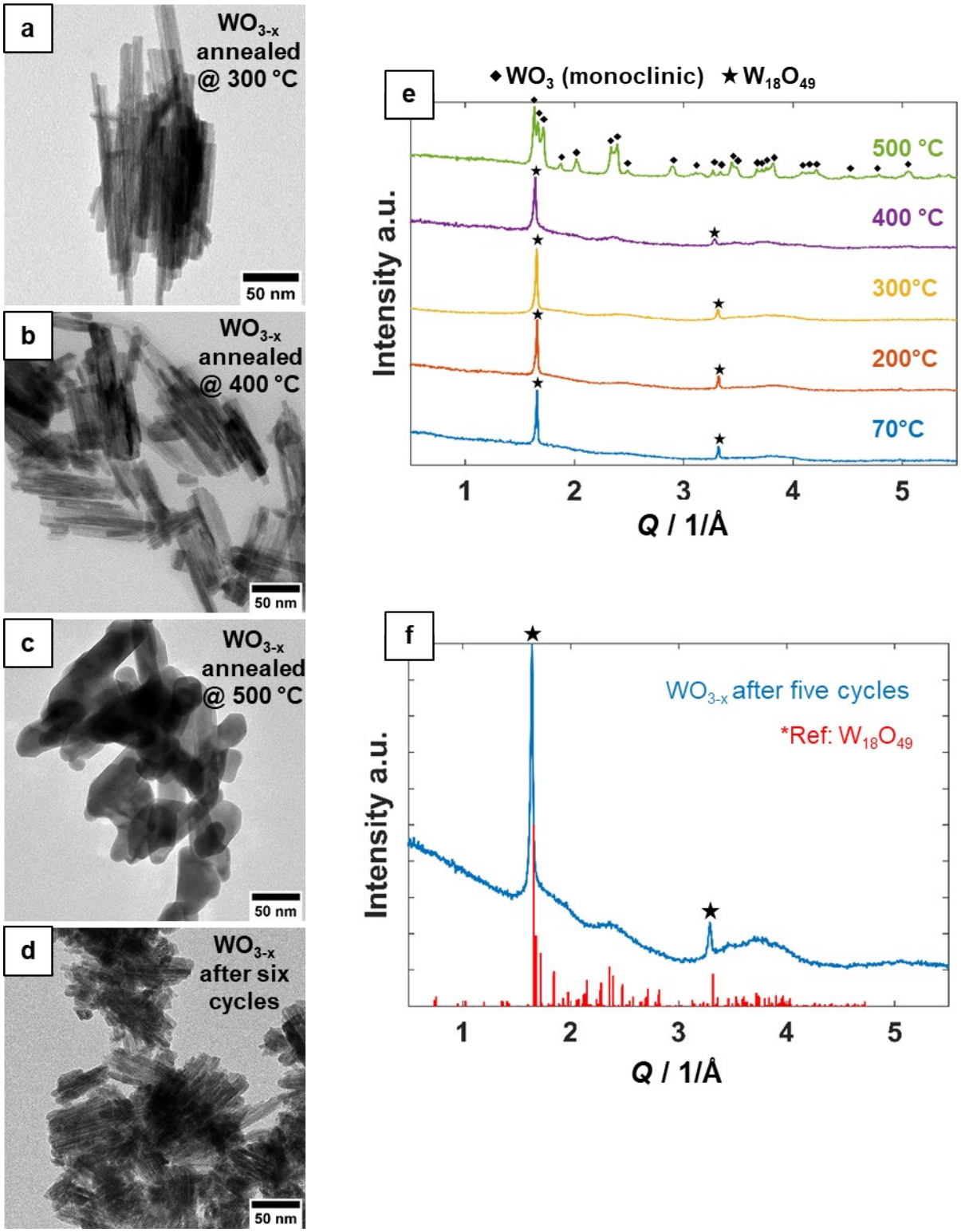

Fig. S2. TEM images of WO_{3-x} nanorods annealed at (a) 300 °C, (b) 400 °C, (c) 500 °C and (d) after six reaction cycles. (e) P-XRD patterns of annealed WO_{3-x} nanorods up to 500 °C and (f) after five reaction cycles. References: $W_{18}O_{49}$ ($WO_{2.72}$, COD, Entry No.: 96-152-8167), WO_3 (monoclinic, COD, Entry No.: 96-152-8916).

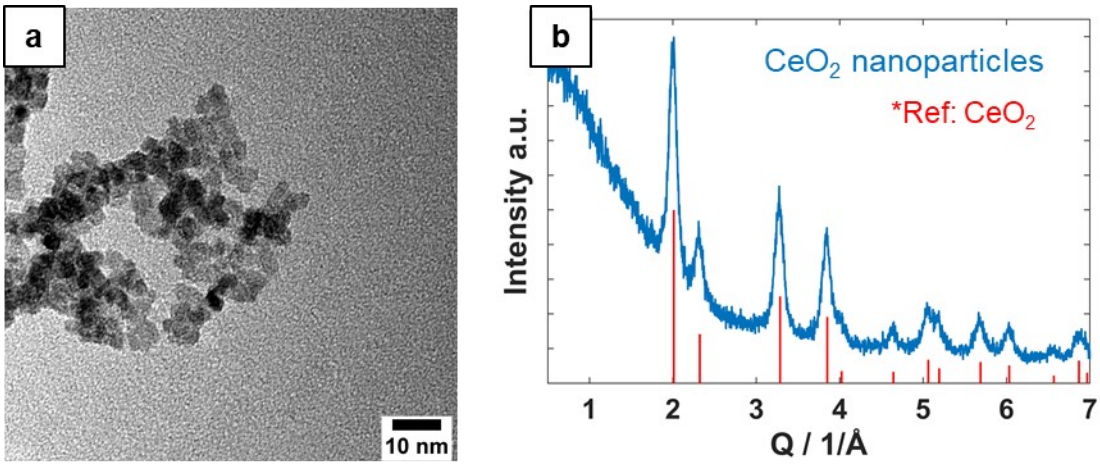

Fig. S3. (a) TEM image and (b) P-XRD pattern of CeO_2 nanoparticles. Reference: Cerianite (CeO_2), COD, Entry No.: 96-900-9009).

^{1}H-NMR characterization

Thioanisole (methyl phenyl sulfide)

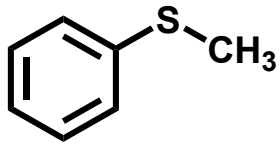

^{1}H-NMR (400 MHz, d_4-MeOD) δ (ppm): 7.29-7.26 (m, 4H), 7.15-7.12 (m,1H) 2.48 (s, 3H).
Published elsewhere[5]: **^{1}H-NMR** (400 MHz, $CDCl_3$) δ (ppm): 7.32-7.20 (m, 4H), 7.17-7.07 (m, 1H), 2.47 (s, 3H).

Methyl phenyl sulfoxide

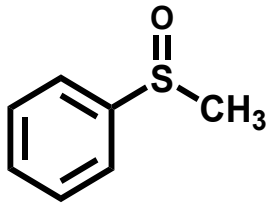

^{1}H-NMR (400 MHz, d_4-MeOD) δ (ppm): 7.74-7.61 (m, 5H), 2.81 (s, 3H).
Published elsewhere[6]: **^{1}H-NMR** (400 MHz, $CDCl_3$) δ (ppm): 7.62-7.60 (m, 2H), 7.51-7.44 (m,3H), 2.68 (s, 3H).

Methyl phenyl sulfone

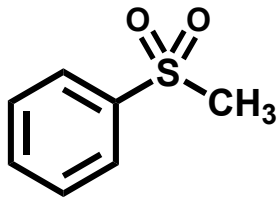

^{1}H-NMR (400 MHz, d_4-MeOD) δ (ppm): 7.99-7.95 (m, 2H), ~7.66-7.54 (m, 3H)[a], 3.13 (s, 3H).
Published elsewhere[6]: **^{1}H-NMR** (400 MHz, $CDCl_3$) δ (ppm): 7.92 (d, J = 7.5 Hz, 2H), 7.66-7.54 (m,3H), 3.04 (s, 3H).
a. Signals of the aromatic protons partially overlapping with those of MP-sulfoxide. MP-sulfone content calculated as 2.5 times the integral of the signal at 7.99-7.95 ppm. The MP-sulfoxide contend was calculated as the integral of the signal at 7.62-7.44 ppm minus the 1.5 times the integral of the signal at 7.99-7.95 ppm.

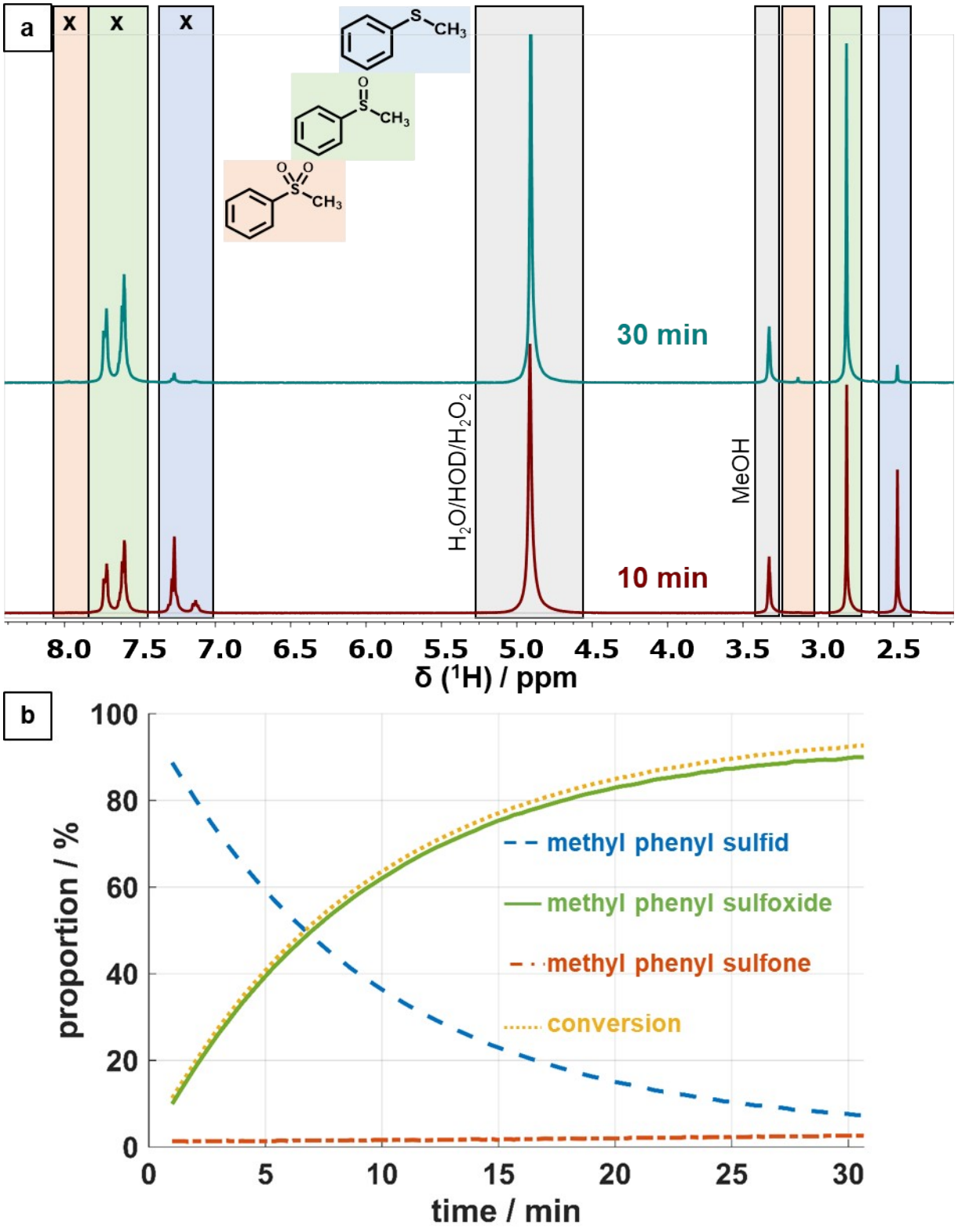

Fig. S4. (a) ^{1}H-NMR spectra of a standard catalysis (0.04 mmol thioanisole, 0.06 mmol H_2O_2 (60 %), 0.85 mg WO_{3-x} nanorods in 0.6 mL of methanol-d_4) after 10 and 30 min, **x** marking the peaks used for integration. (b) Time dependent composition during the catalysis based on ^{1}H-NMR data.

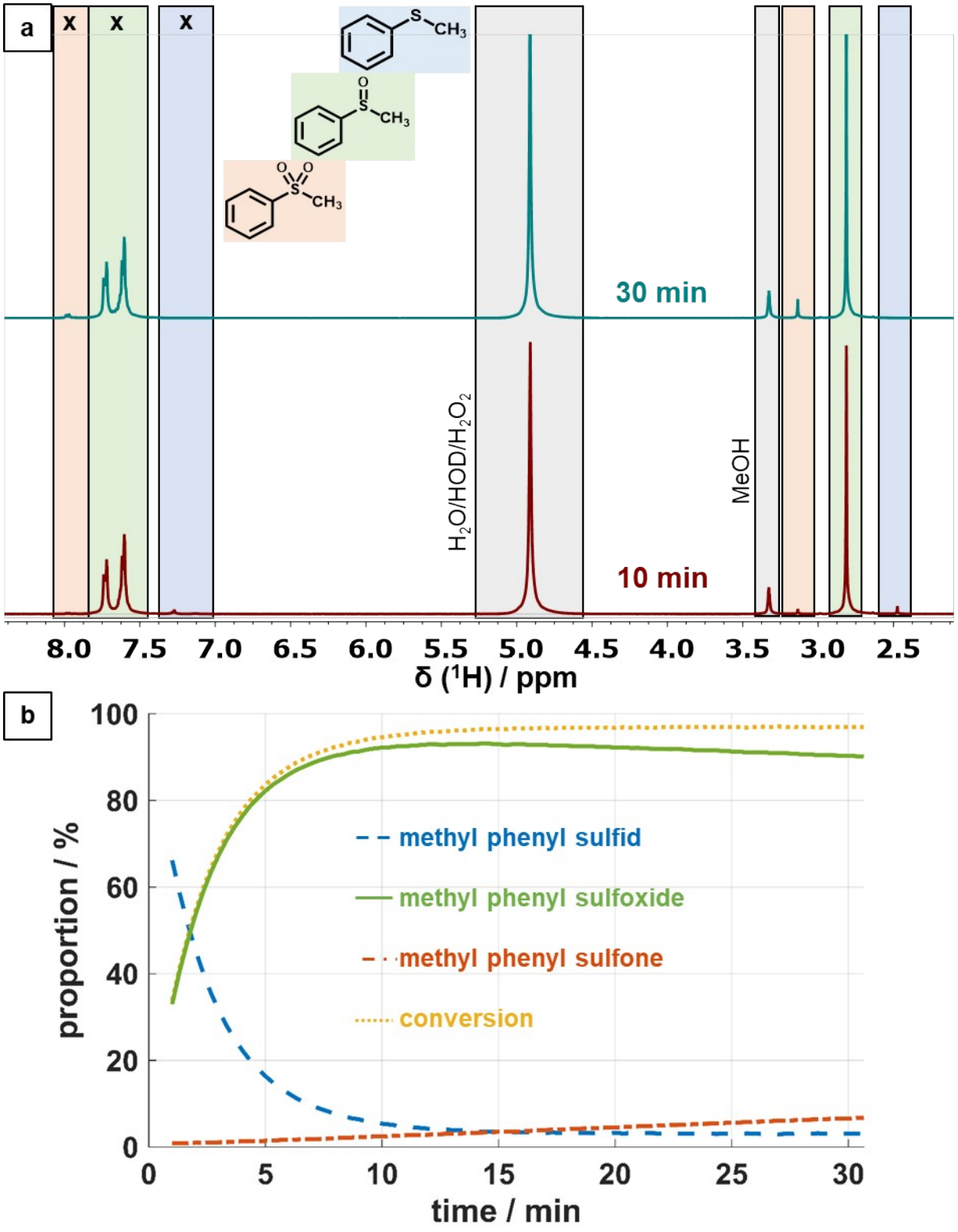

Fig. S5. (a) ^{1}H-NMR spectra of a catalysis with double amounts (0.08 mmol thioanisole, 0.12 mmol H_2O_2 (60 %), 1.7 mg WO_{3-x} nanorods in 0.6 mL of methanol-d_4) after 10 and 30 min, **x** marking the peaks used for integration. (b) Time dependent composition during the catalysis based on ^{1}H-NMR data.

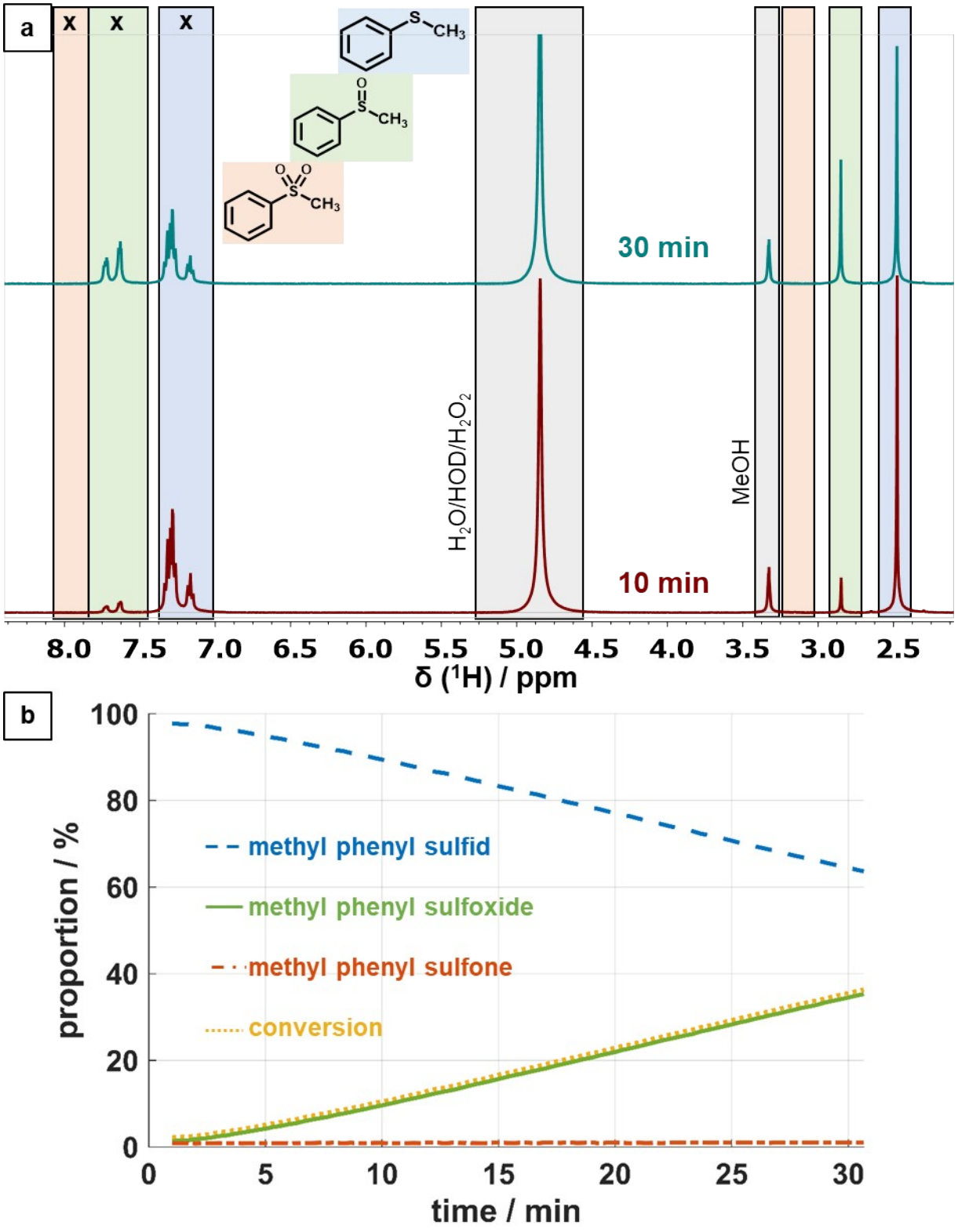

Fig. S6. (a) ^{1}H-NMR spectra of a catalysis with water influence (0.04 mmol thioanisole, 0.06 mmol H_2O_2 (60 %), 0.85 mg WO_{3-x} nanorods in 0.4 mL of methanol-d_4 and 0.2 ml D_2O) after 10 and 30 min, **x** marking the peaks used for integration. (b) Time-dependent composition during the catalysis based on ^{1}H-NMR data.

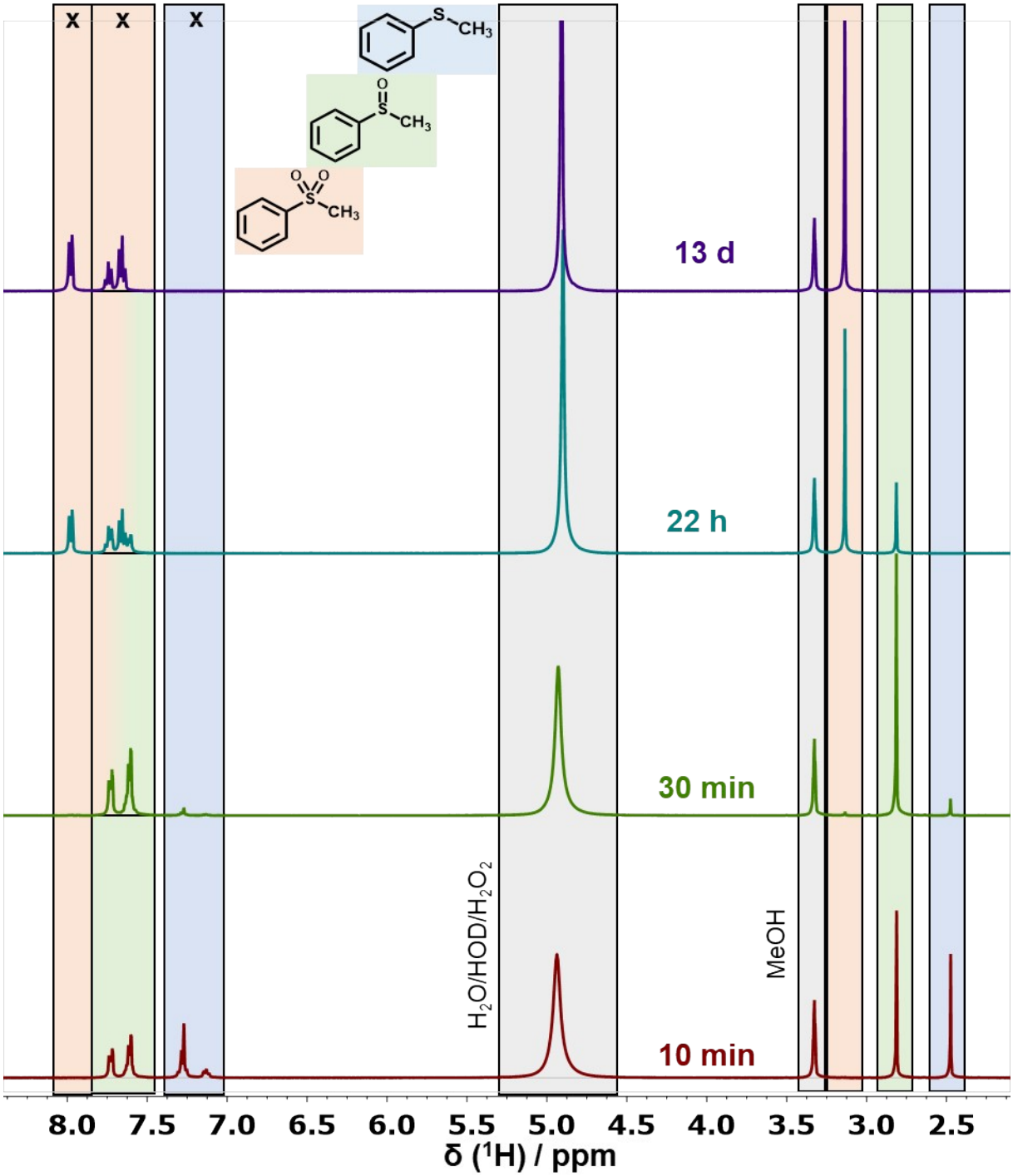

Fig. S7. ^{1}H-NMR spectra of a standard catalysis (0.04 mmol thioanisole, 0.12 mmol H_2O_2 (60 %), 0.85 mg WO_{3-x} nanorods in 0.6 mL of methanol-d_4) after 10 min, 30 min, 22h and 13 d, **x** marking the peaks used for integration.

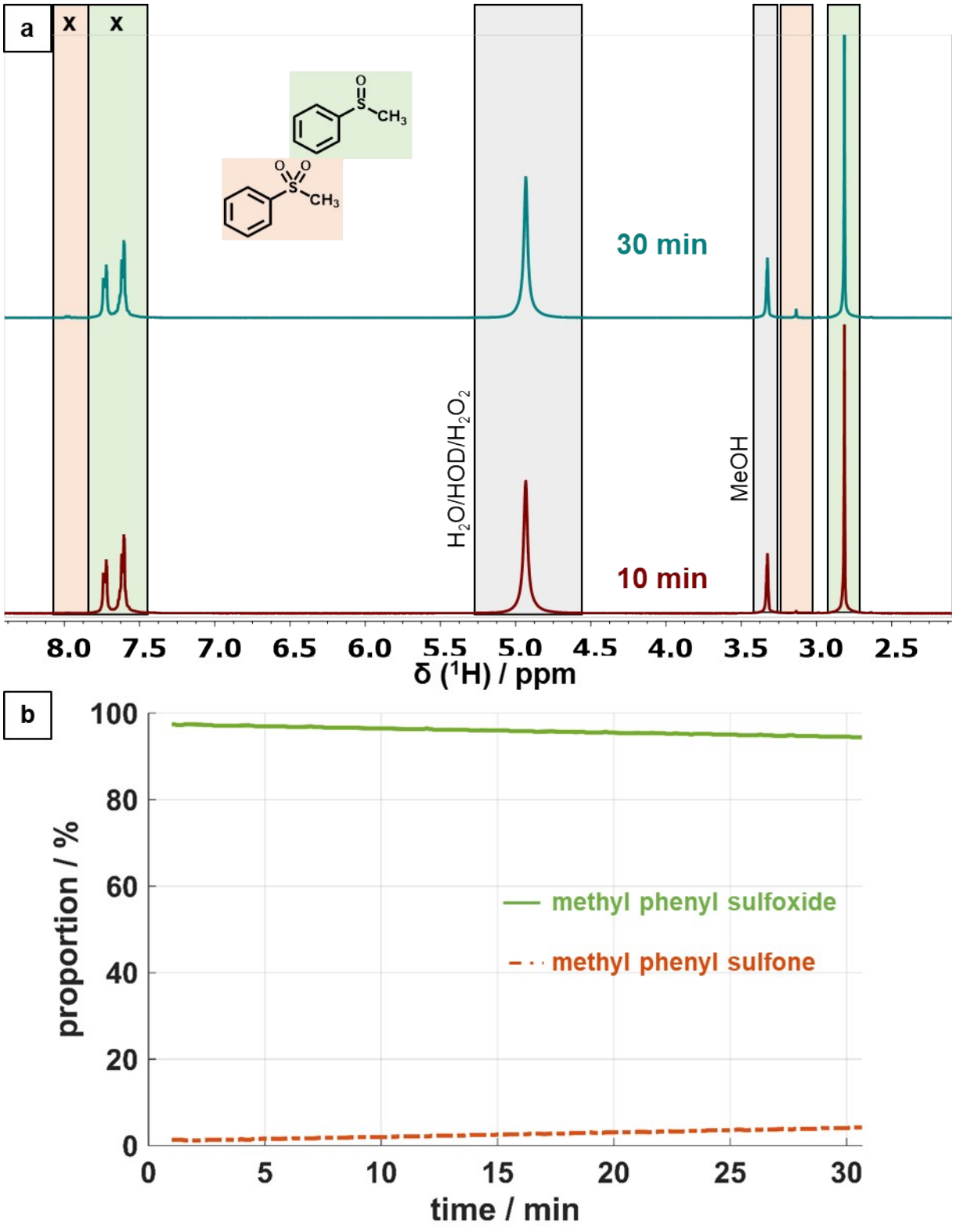

Fig. S8. (a) ^{1}H-NMR spectra of an oxidation catalysis using sulfoxides (0.04 mmol MP-sulfone, 0.06 mmol H_2O_2 (60 %), 0.85 mg WO_{3-x} nanorods in 0.6 mL of methanol-d_4) after 10 and 30 min, **x** marking the peaks used for integration. (b) Time-dependent composition during the catalysis based on ^{1}H-NMR data.

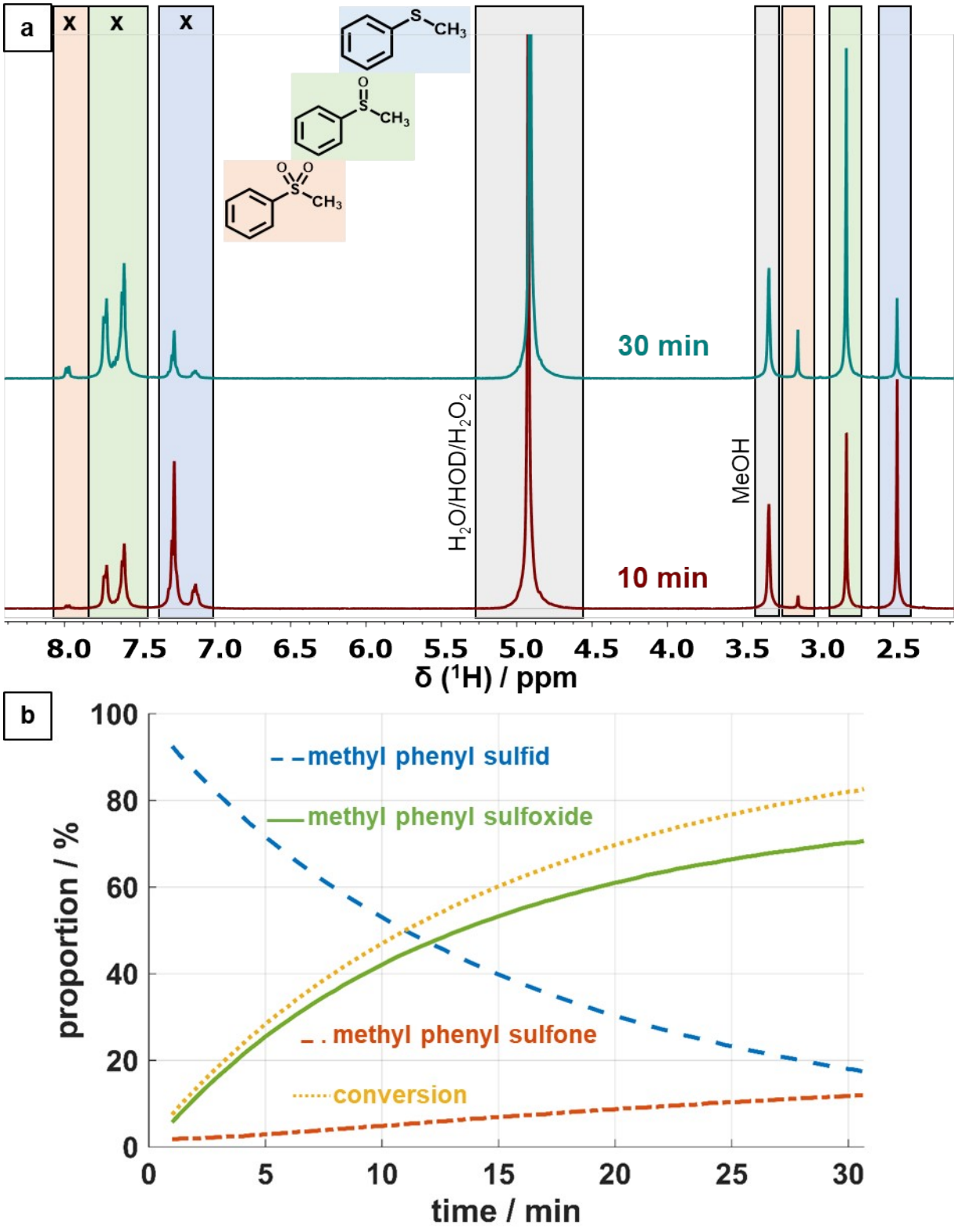

Fig. S9. (a) ^{1}H-NMR spectra of a standard oxidation catalysis (0.04 mmol thioanisole, 0.06 mmol H_2O_2 (60 %), 0.85 mg Na_2WO_4 * $2H_2O$ in 0.6 mL of methanol-d_4) after 10 and 30 min, **x** marking the peaks used for integration. (b) Time-dependent composition during the catalysis based on ^{1}H-NMR data.

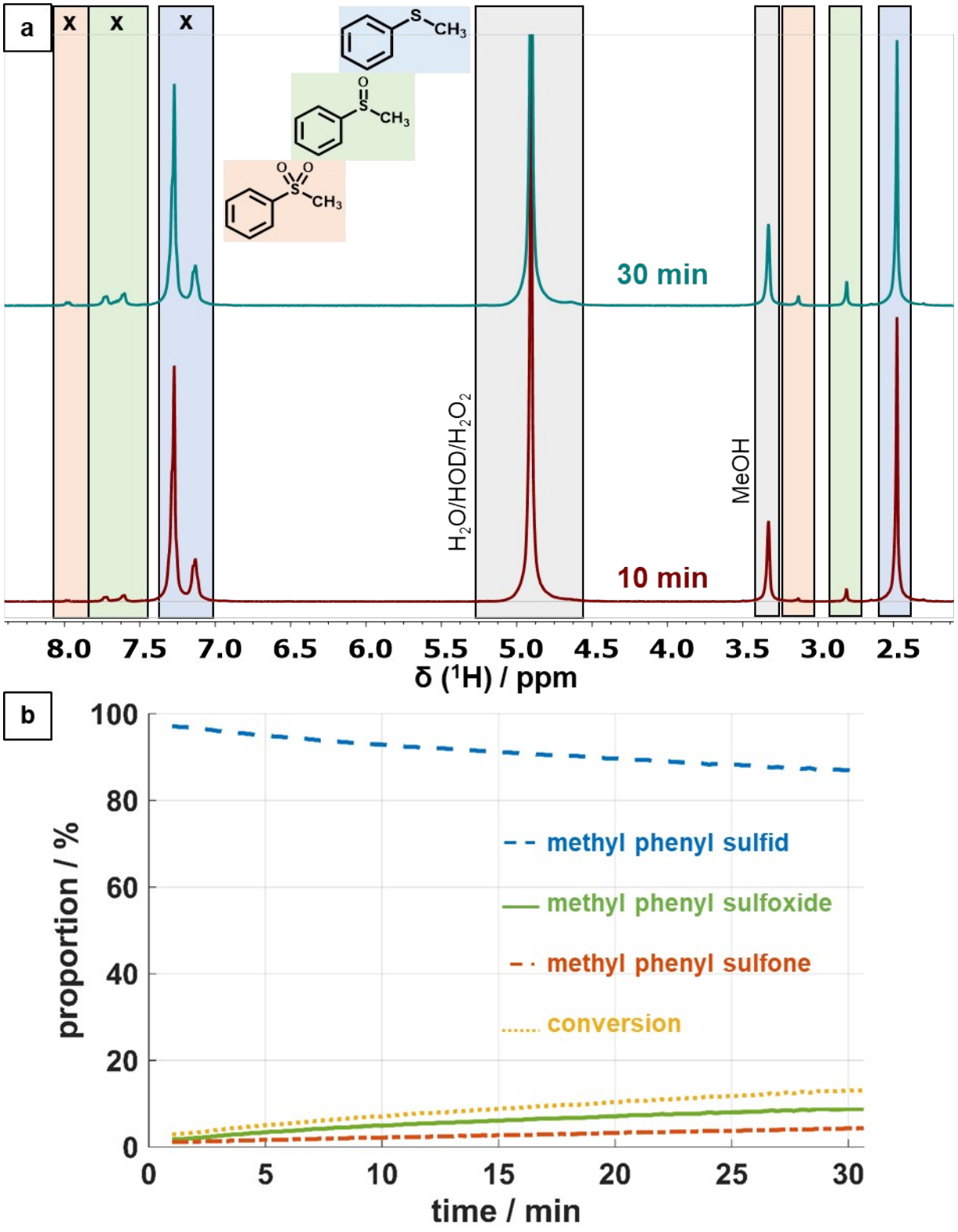

Fig. S10. (a) ^{1}H-NMR spectra of a standard catalysis (0.04 mmol thioanisole, 0.06 mmol H_2O_2 (60 %), 0.85 mg CeO_2 nanoparticles in 0.6 mL of methanol-d_4) after 10 and 30 min, **x** marking the peaks used for integration. (b) Time-dependent composition during the catalysis based on ^{1}H-NMR data.

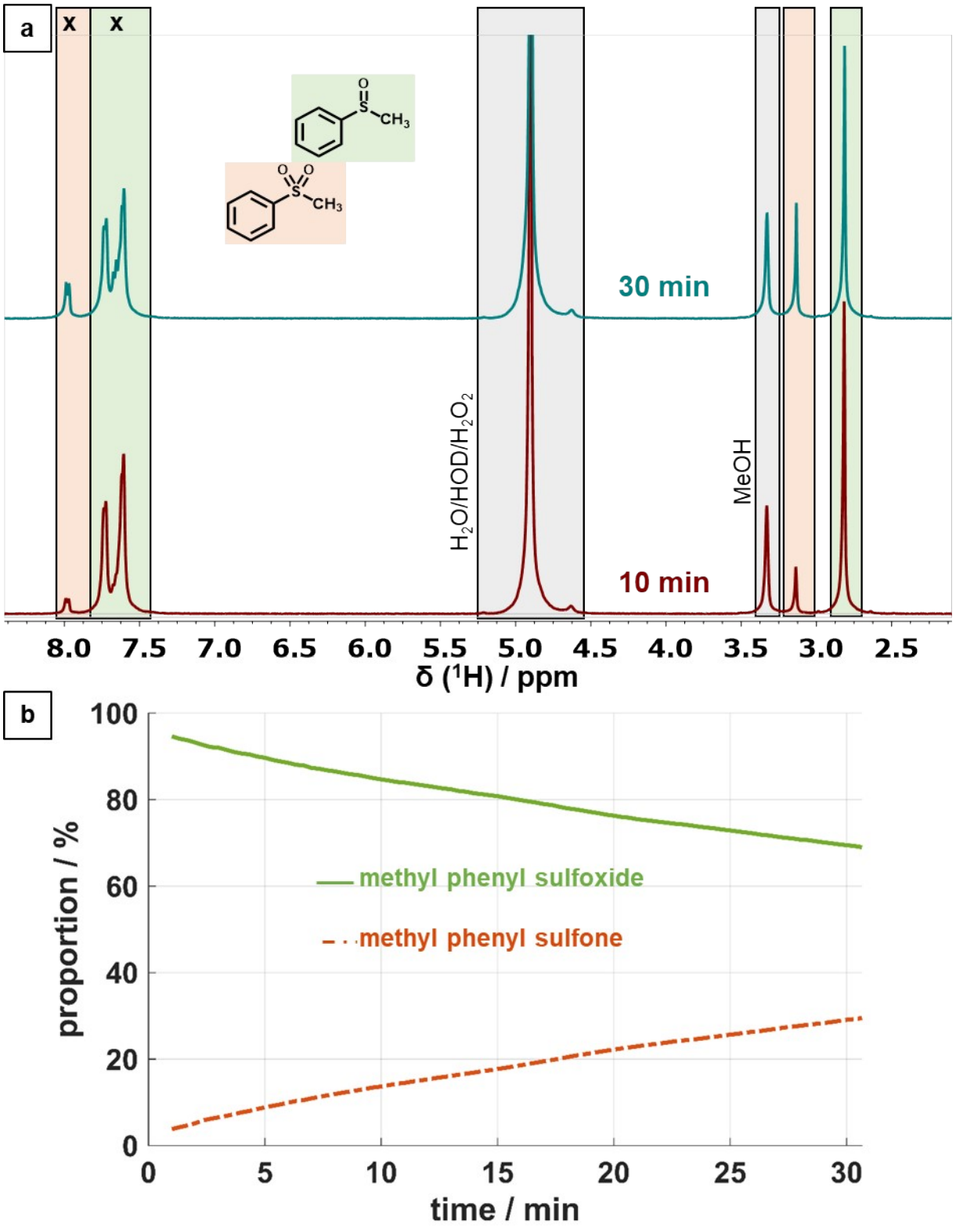

Fig. S11. (a) ^{1}H-NMR spectra of a catalysis using sulfoxide (0.04 mmol MP-sulfoxide, 0.06 mmol H_2O_2 (60 %), 0.85 mg CeO_2 nanoparticles in 0.6 mL of methanol-d_4) after 10 and 30 min, **x** marking the peaks used for integration. (b) Time-dependent composition during the catalysis based on ^{1}H-NMR data.

Di-n-propyl sulfide

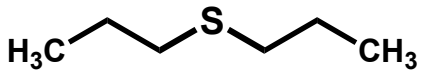

^{1}H-NMR (400 MHz, d_4-MeOD) δ (ppm): 2.49 (t, *J* = 7.2 Hz, 4H), 1.66-1.56 (m, 4H), 1.00 (t, *J* = 7.4 Hz, 6H).

Published elsewhere[7]: **^{1}H-NMR** (400 MHz, $CDCl_3$) δ (ppm): 2.47 (t, *J* = 7.4 Hz, 4H), 1.59 (sext, *J* = 7.4 Hz, 4H), 0.97 (t, *J* = 7.4 Hz, 6H).

Di-n-propyl sulfoxide

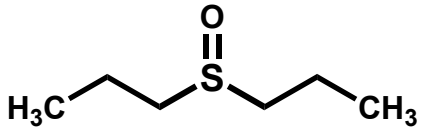

^{1}H-NMR (400 MHz, d_4-MeOD) δ (ppm): 2.83-2.72 (m, 4H), 1.87-1.77 (m, 4H), 1.12 (t, *J* = 7.4 Hz, 6H).

Published elsewhere[6]: **^{1}H-NMR** (400 MHz, $CDCl_3$) δ (ppm): 2.72-2.53 (m, 4H), 1.83-1.73 (m,4H), 1.05 (t, *J* = 7.4 Hz, 6H).

Di-n-propyl sulfone

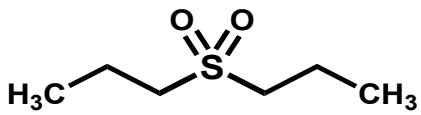

^{1}H-NMR (400 MHz, d_4-MeOD) δ (ppm): 3.07-3.03 (m, 4H), ~1.88-1.75 (m, 4H)[a], ~1.12 (t, *J* = 7.4 Hz, 6H)[a].

Published elsewhere[6]: **^{1}H-NMR** (400 MHz, $CDCl_3$) δ (ppm): 2.90-2.86 (m, 4H), 1.86-1.76 (m,4H), 1.02 (t, *J* = 7.4 Hz, 6H).

a. Signals of the protons partially overlapping with those of di-n-propyl sulfoxide.

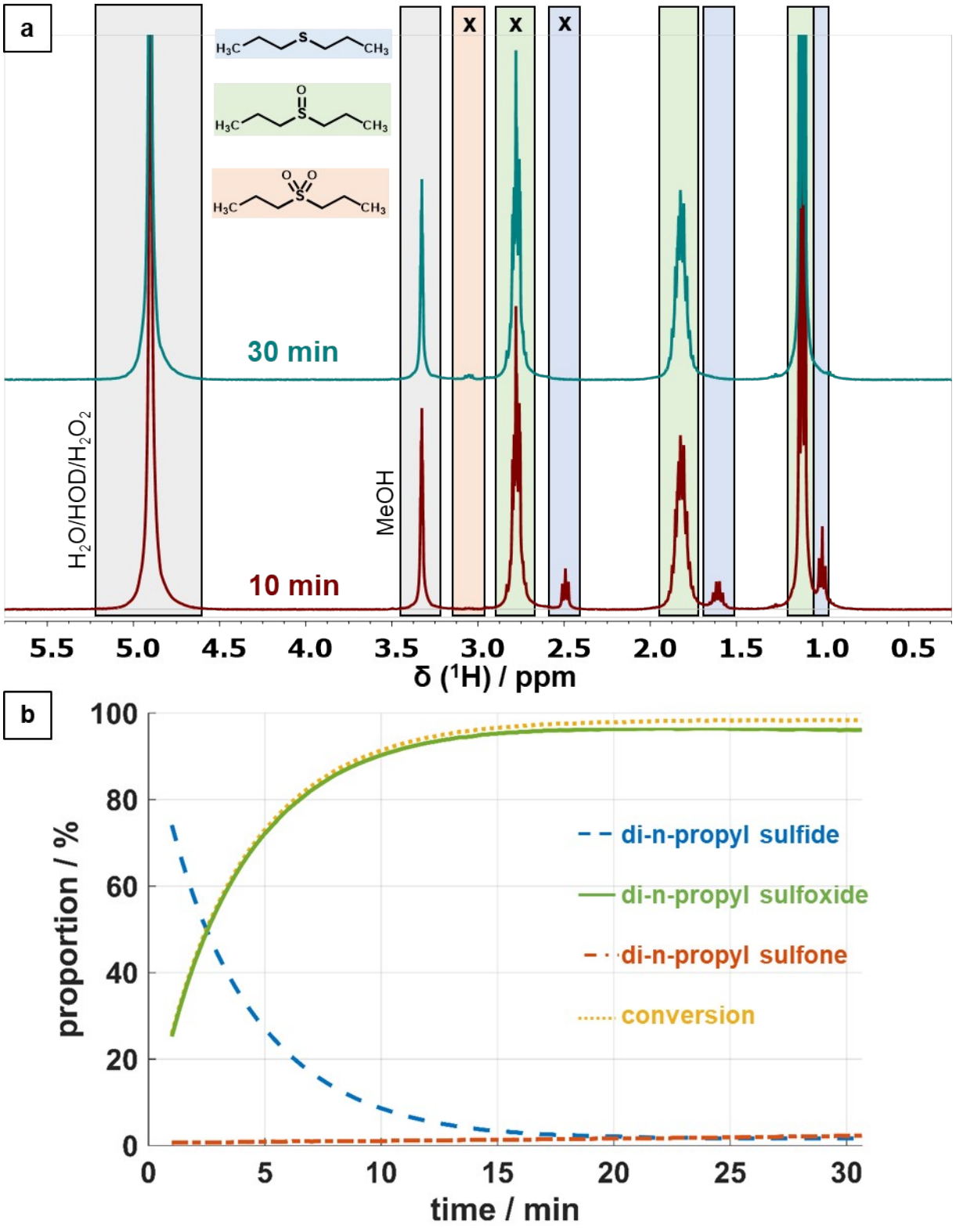

Fig. S12. (a) ^{1}H-NMR spectra of a standard catalysis (0.04 mmol di-n-propyl sulfide, 0.06 mmol H_2O_2 (60 %), 0.85 mg WO_{3-x} nanorods in 0.6 mL of methanol-d_4) after 10 and 30 min, **x** marking the peaks used for integration. (b) Time-dependent composition during the catalysis based on ^{1}H-NMR data.

Di-tert-butyl sulfide

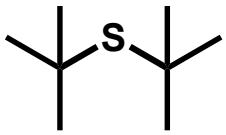

^{1}H-NMR (400 MHz, d_4-MeOD) δ (ppm): 1.42 (s, 18H).

Published elsewhere[8]: **^{1}H-NMR** (400 MHz, $CDCl_3$) δ (ppm): 1.42 (s, 18H).

Di-tert-butyl sulfoxide

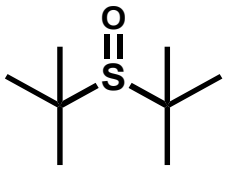

^{1}H-NMR (400 MHz, d_4-MeOD) δ (ppm): 1.37 (s, 18H).

Published elsewhere[9]: **^{1}H-NMR** (400 MHz, $CDCl_3$) δ (ppm): 1.12 (s, 18H).

Di-tert-butyl sulfone

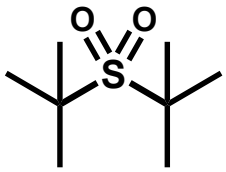

Not observed.

Published elsewhere[9]: **^{1}H-NMR** (400 MHz, $CDCl_3$) δ (ppm): 1.31 (s, 18H).

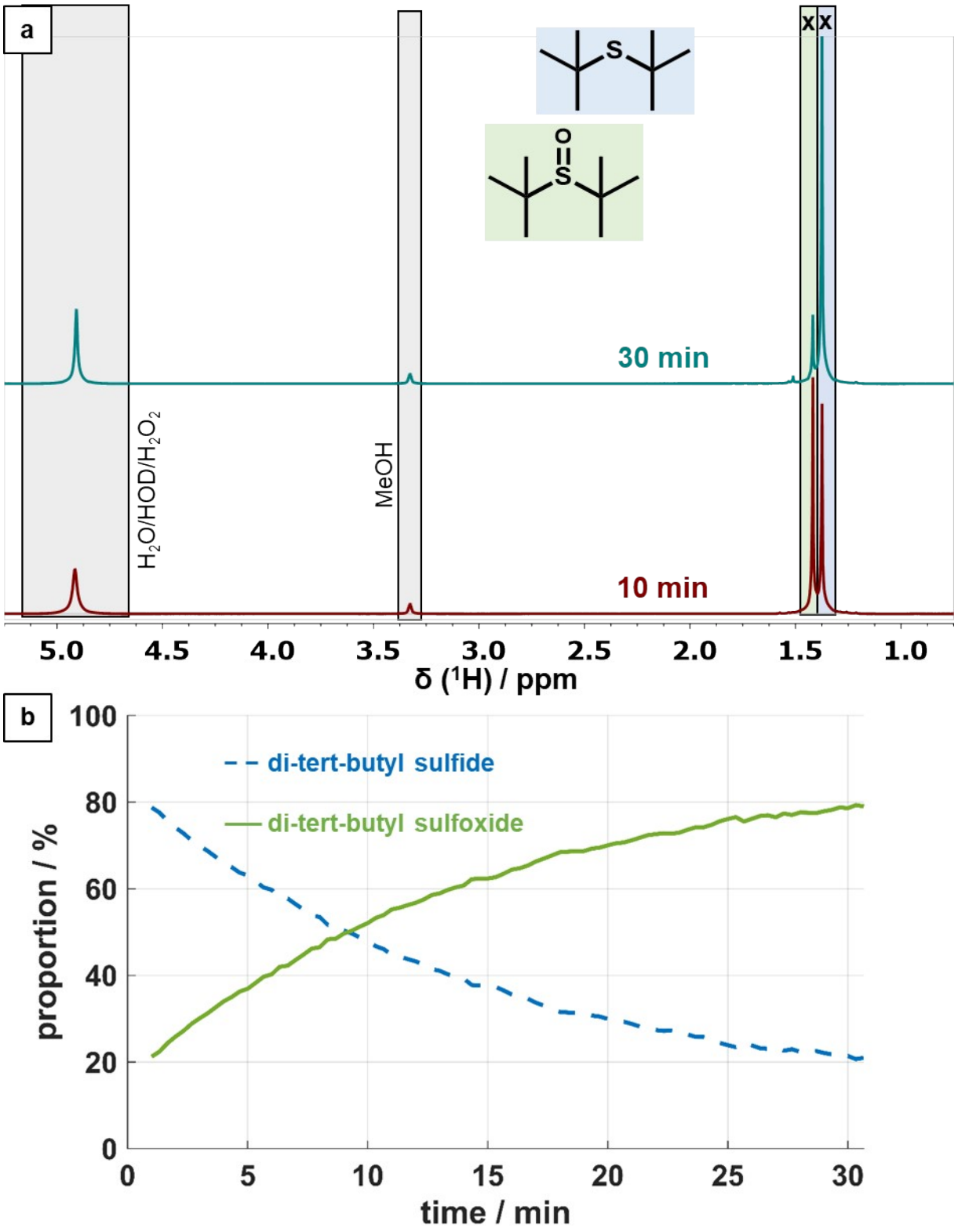

Fig. S13. (a) ^{1}H-NMR spectra of a standard catalysis (0.04 mmol di-tert-butyl sulfide, 0.06 mmol H_2O_2 (60 %), 0.85 mg WO_{3-x} nanorods in 0.6 mL of methanol-d_4) after 10 and 30 min, **x** marking the peaks used for integration. (b) Time-dependent composition during the catalysis based on ^{1}H-NMR data.

Diphenyl sulfide

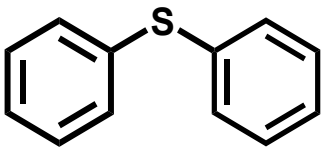

^{1}H-NMR (400 MHz, d_4-MeOD) δ (ppm): 7.33-7.24 (m, 10H).

Published elsewhere[5]: **^{1}H-NMR** (400 MHz, $CDCl_3$) δ (ppm): 7.39 (d, *J* = 7.4 Hz, 4H), 7.34 (dd, *J* = 9.9, 4.8 Hz, 4H), 7.28 (dd, *J* = 7.6, 5.1 Hz, 2H).

Diphenyl sulfoxide

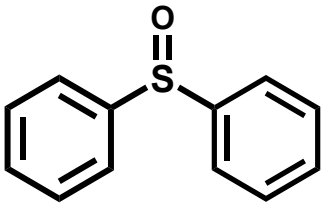

^{1}H-NMR (400 MHz, d_4-MeOD) δ (ppm): 7.72-7.69 (m, 4H), 7.55-7.53 (m, 6H).

Published elsewhere[6]: **^{1}H-NMR** (400 MHz, $CDCl_3$) δ (ppm): 7.66-7.64 (m, 4H), 7.49-7.42 (m, 6H).

Diphenyl sulfone

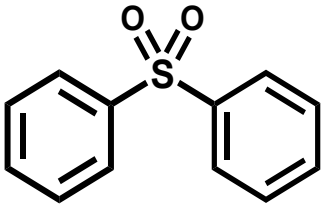

Not observed.

Published elsewhere[6]: **^{1}H-NMR** (400 MHz, $CDCl_3$) δ (ppm): 7.96-7.94 (m, 4H), 7.59-7.49 (m, 6H).

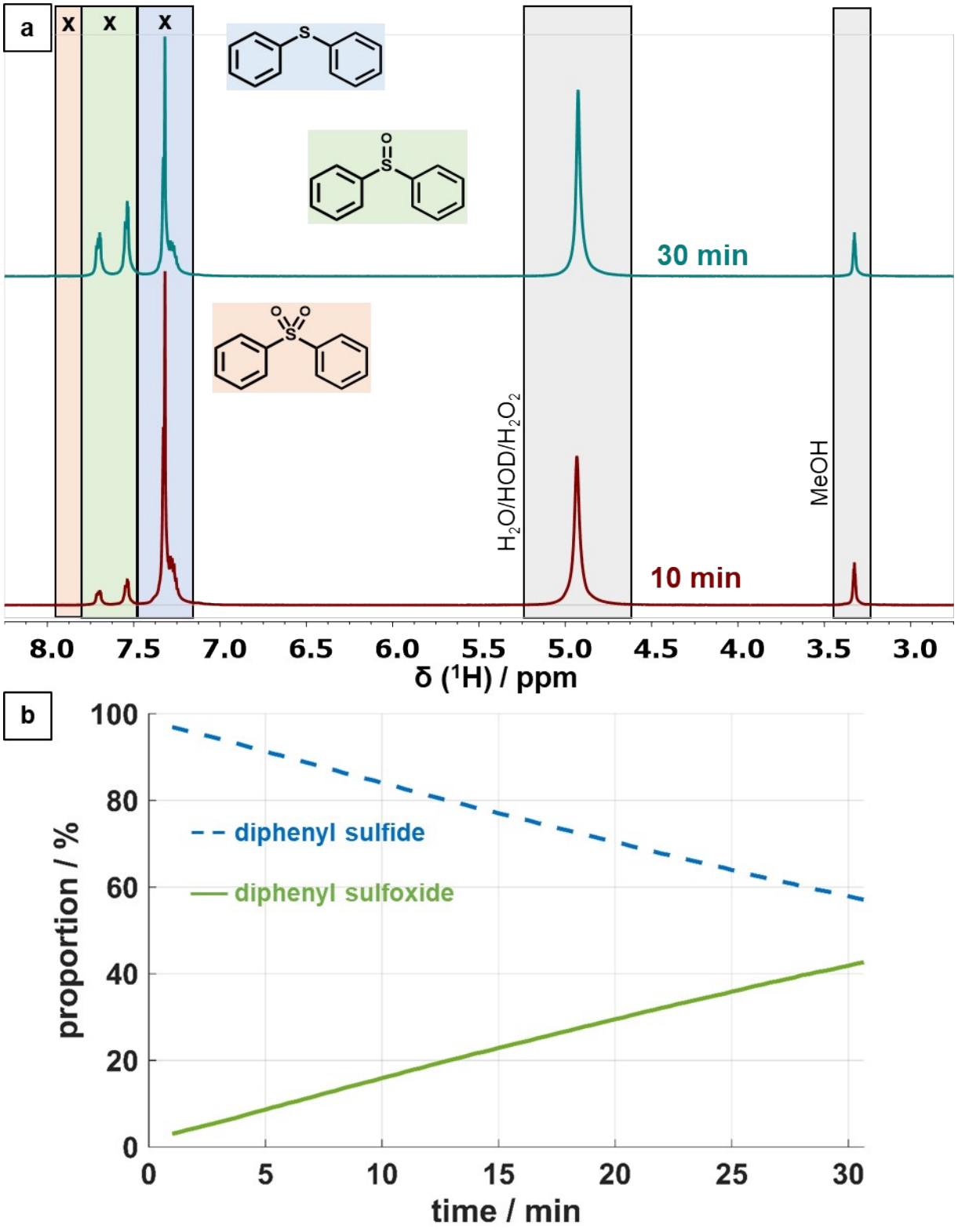

Fig. S14. (a) ^{1}H-NMR spectra of a standard catalysis (0.04 mmol diphenyl sulfide, 0.06 mmol H_2O_2 (60 %), 0.85 mg WO_{3-x} nanorods in 0.6 mL of methanol-d_4) after 10 and 30 min, **x** marking the peaks used for integration. (b) Time-dependent composition during the catalysis based on ^{1}H-NMR data.

Dibenzyl sulfide

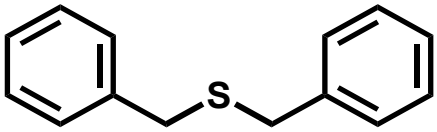

^{1}H-NMR (400 MHz, d_4-MeOD) δ (ppm): 7.31-7.23 (m, 10H), 3.61 (s, 4H).

Published elsewhere[10]: **^{1}H-NMR** (400 MHz, $CDCl_3$) δ (ppm): 7.26-7.14 (m, 10H), 3.55 (s, 4H).

Dibenzyl sulfoxide

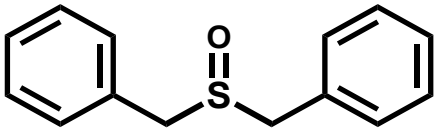

^{1}H-NMR (400 MHz, d_4-MeOD) δ (ppm): 7.41-7.36 (m, 10H), 4.20 (d, J = 13.0, 2H), 3.98 (d, J = 13.0, 2H).

Published elsewhere[6]: **^{1}H-NMR** (400 MHz, $CDCl_3$) δ (ppm): 7.38-7.24 (m, 10H), 3.91 (d, J = 12.0, 2H), 3.86 (d, J = 12.0, 2H).

Dibenzyl sulfone

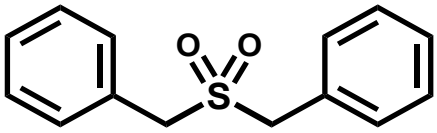

^{1}H-NMR (400 MHz, d_4-MeOD) δ (ppm): 7.60-7.55 (m, 10H), 4.38 (s, 4H).

Published elsewhere[11]: **^{1}H-NMR** (400 MHz, $CDCl_3$) δ (ppm): 7.40-7.46 (m, 10H), 4.16 (s, 4H).

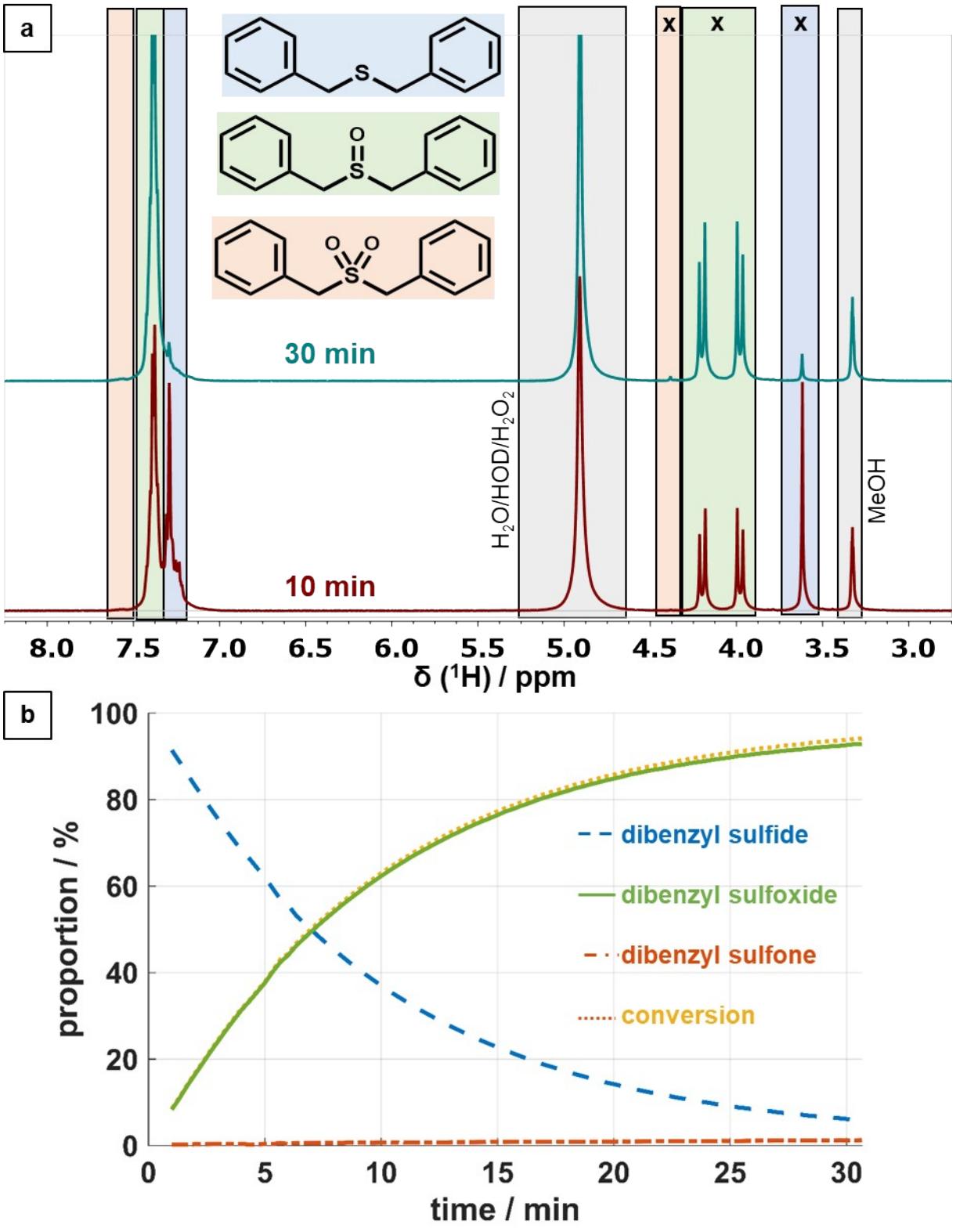

Fig. S15. a) ^{1}H-NMR spectra of a standard catalysis (0.04 mmol dibenzyl sulfide, 0.06 mmol H_2O_2 (60 %), 0.85 mg WO_{3-x} nanorods in 0.6 mL of methanol-d_4) after 10 and 30 min, **x** marking the peaks used for integration. (b) Time-dependent composition during the catalysis based on ^{1}H-NMR data.

4-Nitrothioanisole (4-nitrophenyl methyl sulfide)

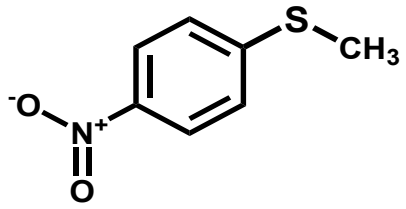

^{1}H-NMR (400 MHz, d_4-MeOD) δ (ppm): 8.16 (d, *J* = 9.0 Hz, 2H), 7.42 (d, *J* = 9.0 Hz, 2H), 2.59 (s, 3H).

Published elsewhere[12]: **^{1}H-NMR** (400 MHz, $CDCl_3$) δ (ppm): 8.24-8.04 (m, 2H), 7.34-7.14 (m, 2H), 2.54 (s, 3H).

4-Nitrophenyl methyl sulfoxide

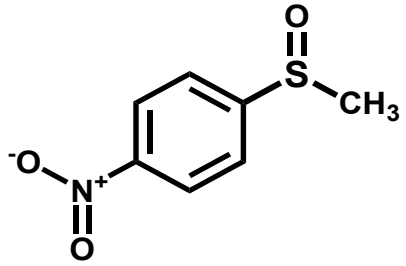

^{1}H-NMR (400 MHz, d_4-MeOD) δ (ppm): 8.45 (d, *J* = 8.9 Hz, 2H), 7.96 (d, *J* = 8.9 Hz, 2H), 2.89 (s, 3H).

Published elsewhere[13]: **^{1}H-NMR** (300 MHz, $CDCl_3$) δ (ppm): 8.36 (d, *J* = 8.7 Hz, 2H), 7.82 (d, *J* = 8.7 Hz, 2H), 2.78 (s, 3H).

4-Nitrophenyl methyl sulfone

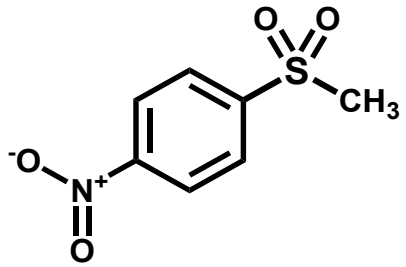

Not observed.

Published elsewhere[13]: **^{1}H-NMR** (300 MHz, $CDCl_3$) δ (ppm): 8.43 (d, *J* = 8.8 Hz, 2H), 8.16 (d, *J* = 8.8 Hz, 2H), 3.12 (s, 3H).

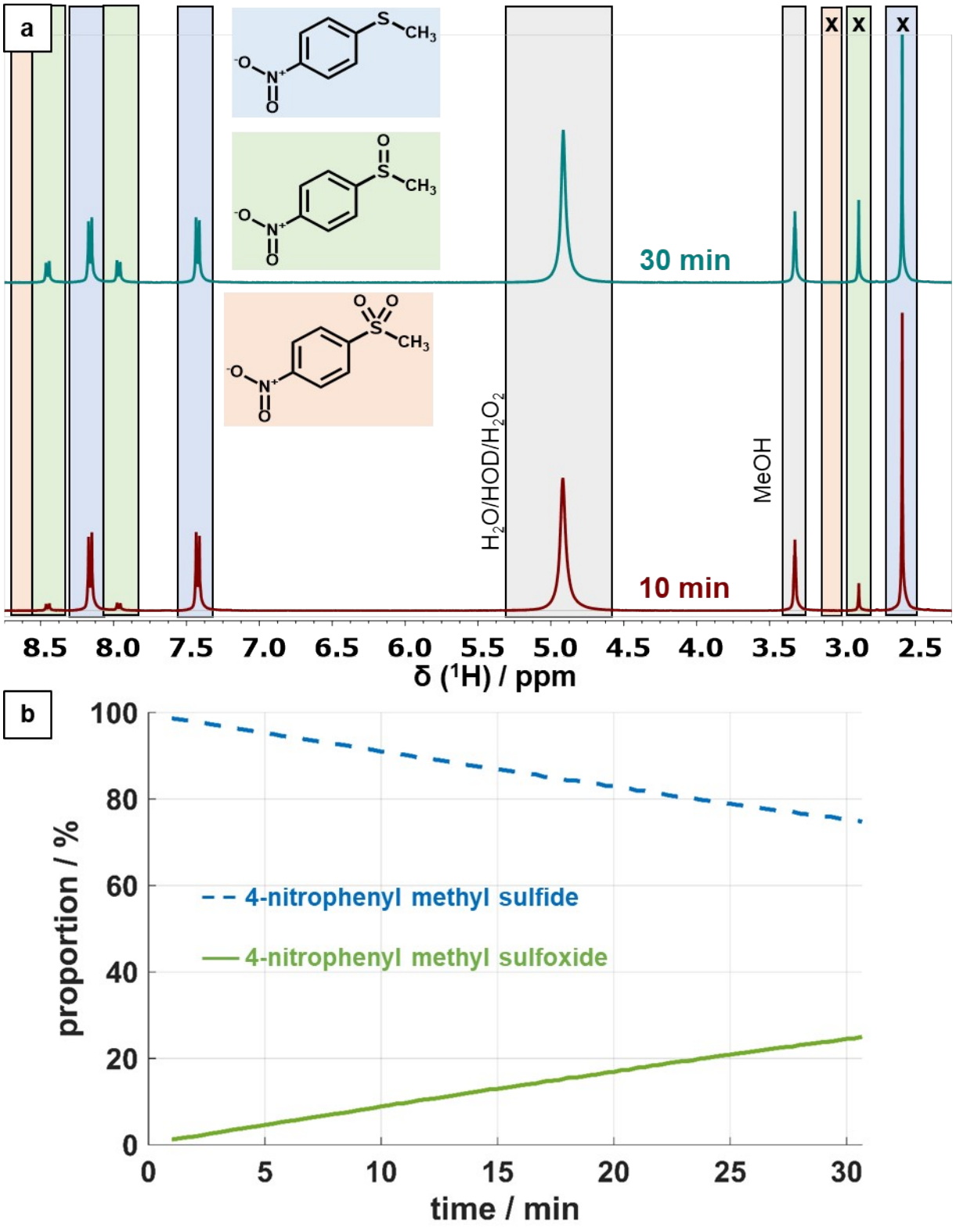

Fig. S16. (a) ^{1}H-NMR spectra of a standard catalysis (0.04 mmol 4-nitrophenyl methyl sulfide, 0.06 mmol H_2O_2 (60 %), 0.85 mg WO_{3-x} nanorods in 0.6 mL of methanol-d_4) after 10 and 30 min, **x** marking the peaks used for integration. (b) Time-dependent composition during the catalysis based on ^{1}H-NMR data.

4-Methoxythioanisole (4-methoxyphenyl methyl sulfide)

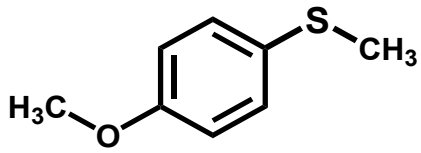

^{1}H-NMR (400 MHz, d_4-MeOD) δ (ppm): 7.27 (d, *J* = 8.8 Hz, 2H), 6.88 (d, *J* = 8.8 Hz,2H), 3.78 (s, 3H), 2,42 (s, 3H).

Published elsewhere[5]: **^{1}H-NMR** (400 MHz, $CDCl_3$) δ (ppm): 7.23 (d, *J* = 8.6 Hz, 2H), 6.81 (d, *J* = 8.6 Hz,2H), 3.75 (s, 3H), 2,40 (s, 3H).

4-Methoxyphenyl methyl sulfoxide

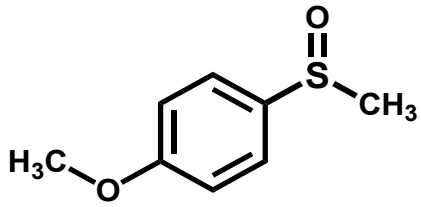

^{1}H-NMR (400 MHz, d_4-MeOD) δ (ppm): 7.68 (d, *J* = 8.7 Hz, 2H), 7.15 (d, *J* = 8.7 Hz, 2H), 3.88 (s, 3H), 2,79 (s, 3H).

Published elsewhere[13]: **^{1}H-NMR** (300 MHz, $CDCl_3$) δ (ppm): 7.53-7.58 (m, 2H), 7.01-6.96 (m, 2H), 3.81 (s, 3H), 2,65 (s, 3H).

4-Methoxyphenyl methyl sulfone

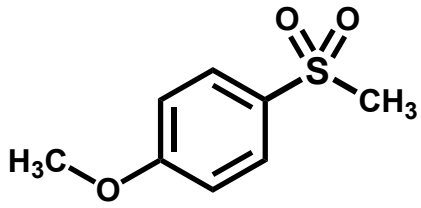

^{1}H-NMR (400 MHz, d_4-MeOD) δ (ppm): 7.89 (d, *J* = 8.4 Hz, 2H), [a](2H), [a](3H), 3.01 (s, 3H).

Published elsewhere[13]: **^{1}H-NMR** (300 MHz, $CDCl_3$) δ (ppm): 7.87 (d, *J* = 8.8 Hz, 2H), 7.02 (d, *J* = 8.8 Hz, 2H), 3.89 (s, 3H), 3.03 (s, 3H).

a. Signal intensity partially too low for assignment.

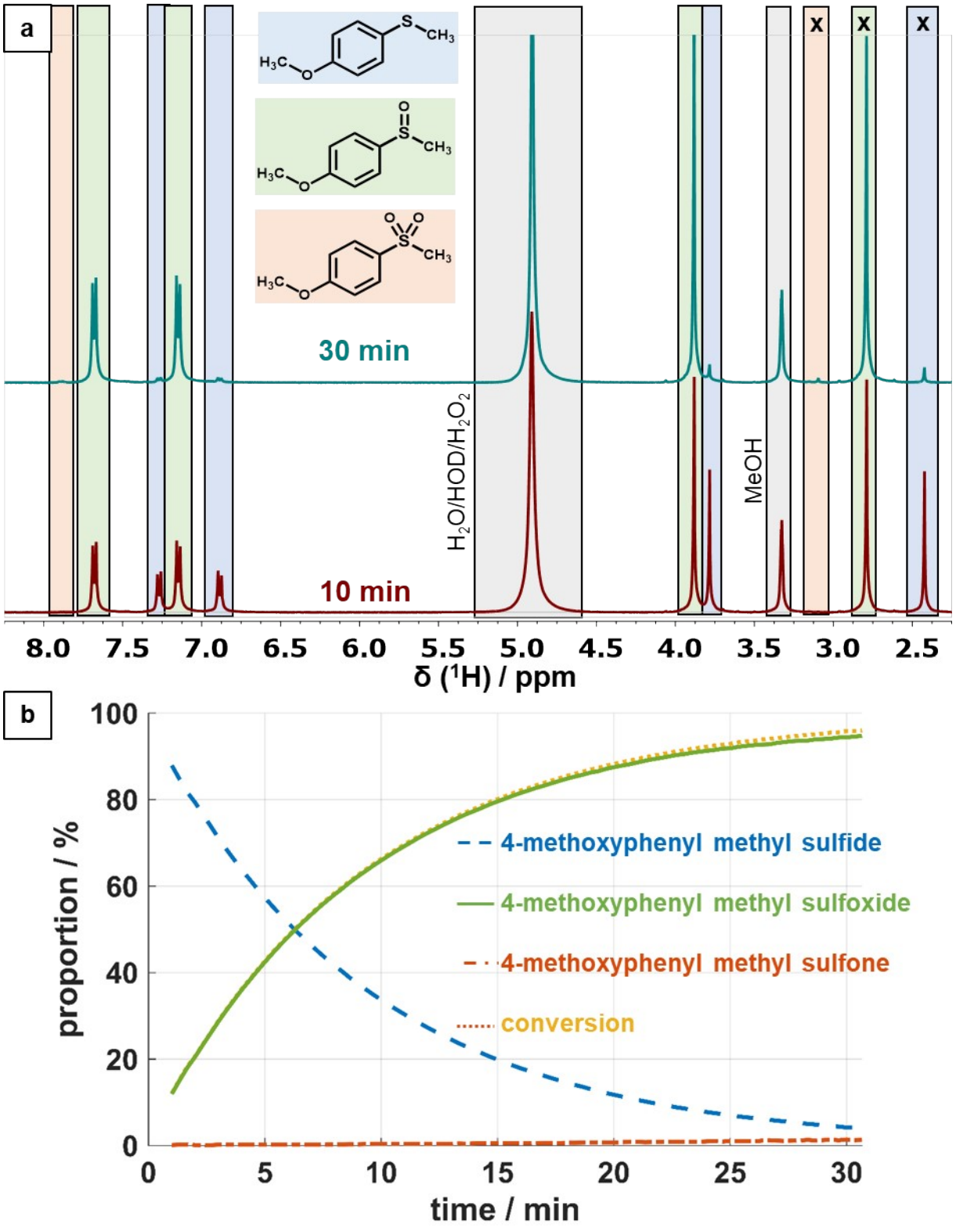

Fig. S17. (a) ^{1}H-NMR spectra of a standard catalysis (0.04 mmol 4-methoxyphenyl methyl sulfide, 0.06 mmol H_2O_2 (60 %), 0.85 mg WO_{3-x} nanorods in 0.6 mL of methanol-d_4) after 10 and 30 min, **x** marking the peaks used for integration. (b) Time-dependent composition during the catalysis based on ^{1}H-NMR data.

4-Aminothioanisole (4-aminophenyl methyl sulfide)

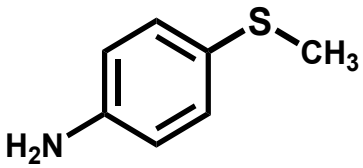

^{1}H-NMR (400 MHz, d_4-MeOD) δ (ppm): 7.14 (d, *J* = 8.6 Hz, 2H), 6.68 (d, *J* = 8.6 Hz, 2H), 2.37 (s, 3H).

Published elsewhere[12]: **^{1}H-NMR** (400 MHz, $CDCl_3$) δ (ppm): 7.21-7.11 (m, 2H), 6.65-6.60 (m, 2H), 3.38 (s, 2H), 2.41 (s, 3H).

4-Aminophenyl methyl sulfoxide

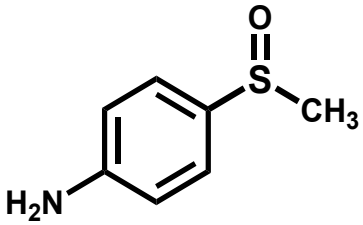

^{1}H-NMR (400 MHz, d_4-MeOD) δ (ppm): 7.46 (d, *J* = 8.7 Hz, 2H), 6.80 (d, *J* = 8.7 Hz, 2H), 2.76 (s, 3H).

Published elsewhere[14]: **^{1}H-NMR** (400 MHz, $CDCl_3$) δ (ppm): 7.45 (d, *J* = 8.8 Hz, 2H), 6.76 (d, *J* = 8.8 Hz, 2H), 3.79 (s, 2H), 2.69 (s, 3H).

4-Aminophenyl methyl sulfone

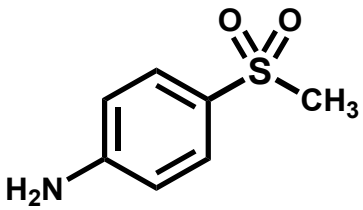

Not observed.

Published elsewhere[15]: **^{1}H-NMR** (400 MHz, $CDCl_3$) δ (ppm): 7.66 (d, *J* = 8.5 Hz, 2H), 6.69 (d, *J* = 8.5 Hz, 2H), 4.26 (s, 2H), 2.99 (s, 3H).

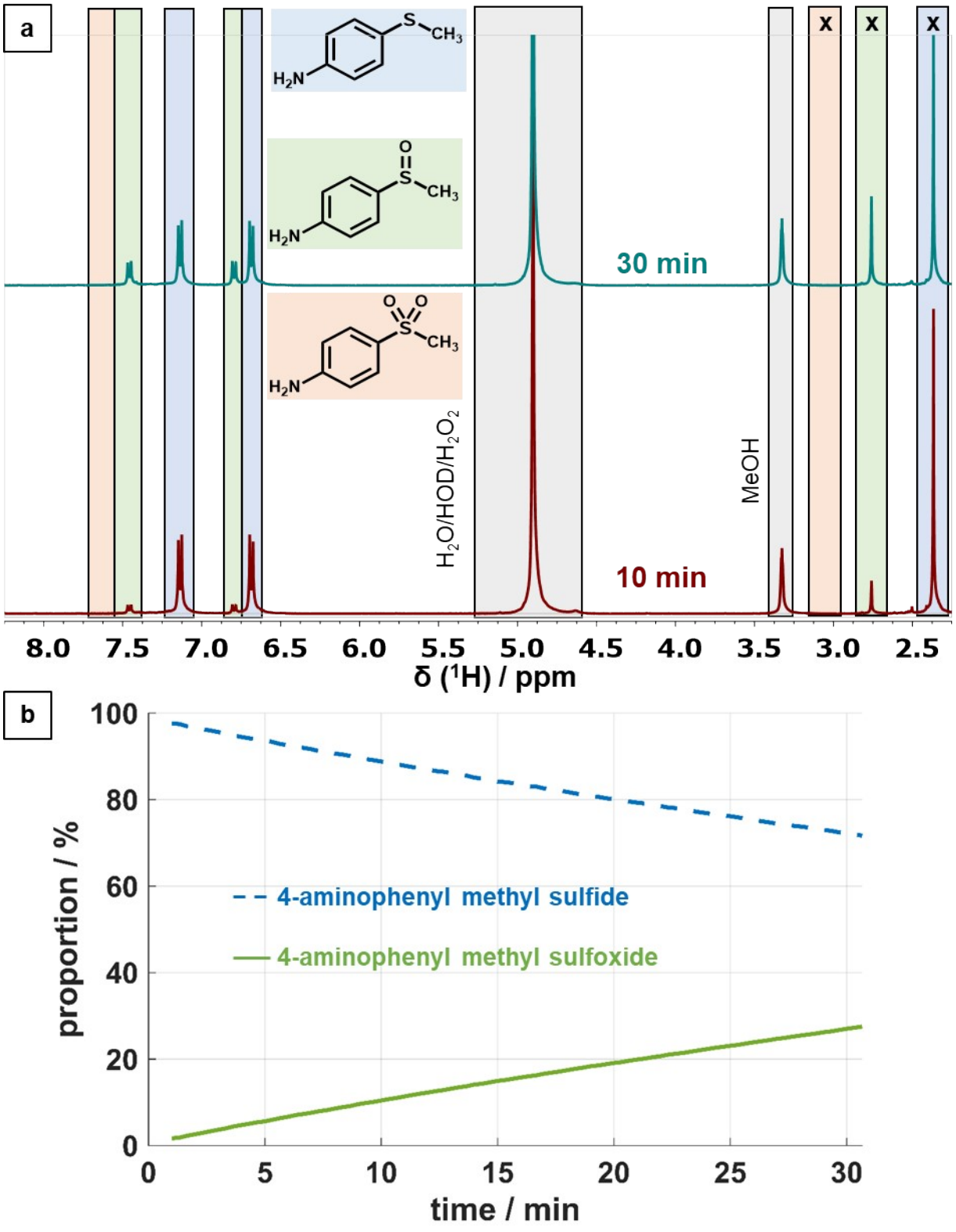

Fig. S18. (a) ^{1}H-NMR spectra of a standard catalysis (0.04 mmol 4-aminophenyl methyl sulfide, 0.06 mmol H_2O_2 (60 %), 0.85 mg WO_{3-x} nanorods in 0.6 mL of methanol-d_4) after 10 and 30 min, **x** marking the peaks used for integration. (b) Time-dependent composition during the catalysis based on ^{1}H-NMR data.

Dimethyl sulfoxide (DMSO)

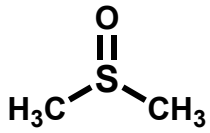

^{1}H-NMR (400 MHz, d_4-MeOD) δ (ppm): 2.68 (s, 3H).

Published elsewhere[16]: **^{1}H-NMR** (400 MHz, $CDCl_3$) δ (ppm): 2.50 (s, 6H).

Dimethyl sulfone

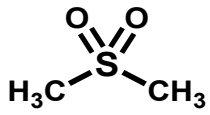

^{1}H-NMR (400 MHz, d_4-MeOD) δ (ppm): 3.03 (s, 3H).

Published elsewhere[16]: **^{1}H-NMR** (400 MHz, $CDCl_3$) δ (ppm): 2.97 (s, 6H).

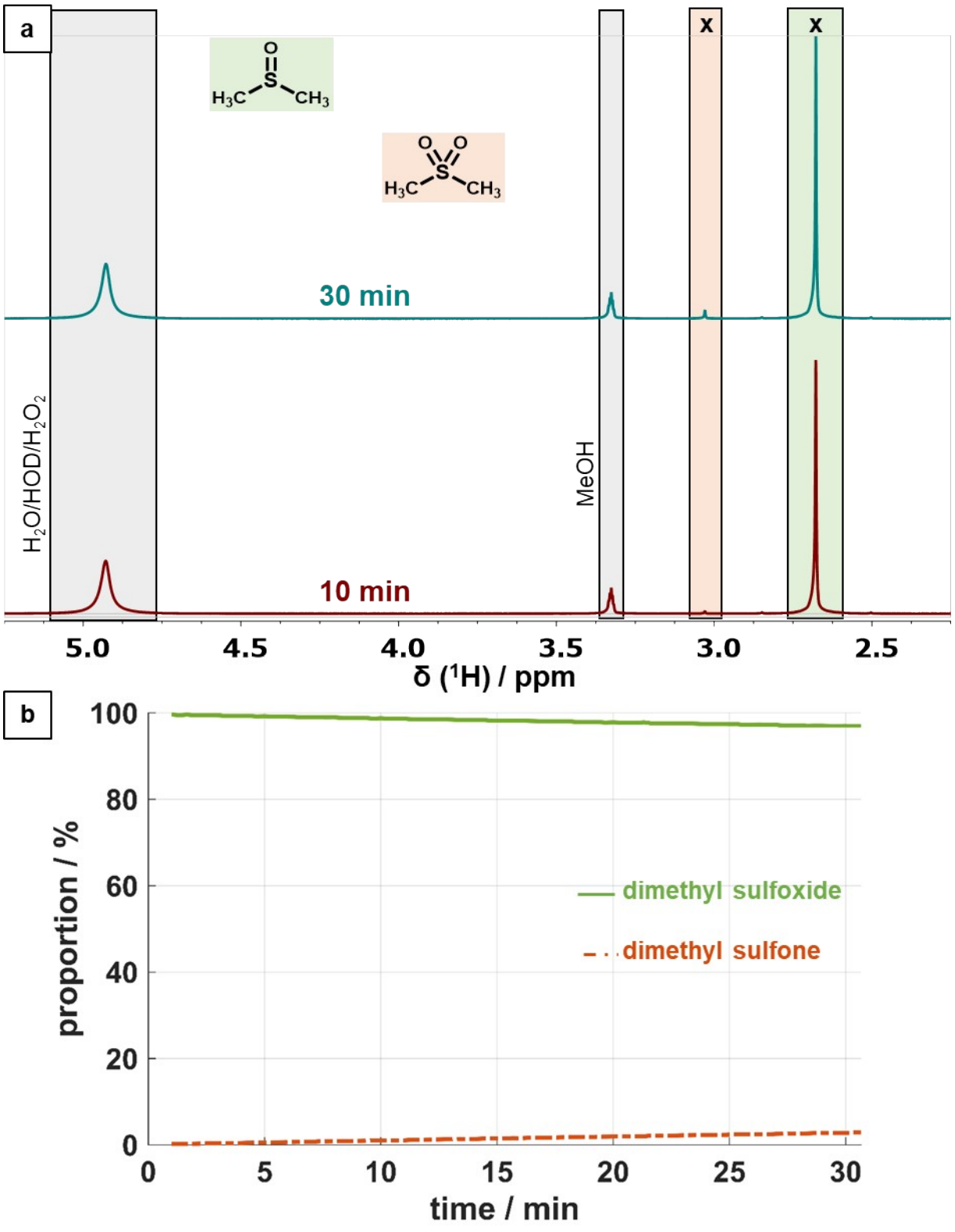

Fig. S19. (a) ^{1}H-NMR spectra of a catalysis using sulfoxides (0.04 mmol DMSO, 0.06 mmol H_2O_2 (60 %), 0.85 mg WO_{3-x} nanorods in 0.6 mL of methanol-d_4) after 10 and 30 min, **x** marking the peaks used for integration. (b) Time-dependent composition during the catalysis based on ^{1}H-NMR data.

Dibenzothiophene (DBT)

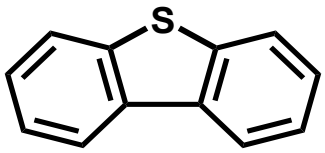

^{1}H-NMR (400 MHz, d_4-MeOD) δ (ppm): 8.27-8.24 (m, 2H), 7.91-7.89 (m, 2H), 7.51-7.49 (m, 4H).

Published elsewhere[17]: **^{1}H-NMR** (400 MHz, $CDCl_3$) δ (ppm): 8.21-8.13 (m, 2H), 7.91-7.82 (m, 2H), 7.51-42 (m, 4H).

Dibenzothiophene sulfoxide

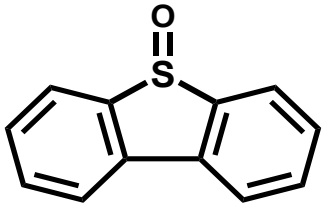

^{1}H-NMR (400 MHz, d_4-MeOD) δ (ppm): 8.05 (dd, *J* = 7.7, 4.3 Hz, 4H), 7.75 (t, *J* = 7.6 Hz, 2H), 7.63 (t, *J* = 7.7 Hz, 2H).

Published elsewhere[16]: **^{1}H-NMR** (400 MHz, $CDCl_3$) δ (ppm): 7.99 (d, *J* = 7.6 Hz, 2H), 7.82 (d. *J* = 7.7 Hz, 2H), 7.61 (t, *J* = 7.5 Hz, 2H), 7.51 (t, *J* = 7.5 Hz, 2H).

Dibenzothiophene sulfone

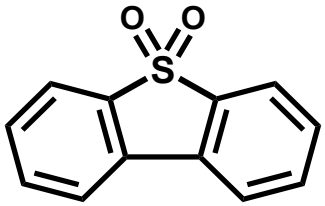

^{1}H-NMR (400 MHz, d_4-MeOD) δ (ppm): 8.08-8.03 (m, 4H), 7.80 (t, *J* = 8.8 Hz, 2H), 7.66 (t, *J* = 8.4 Hz, 2H).

Published elsewhere[16]: **^{1}H-NMR** (400 MHz, $CDCl_3$) δ (ppm): 7.83-7.78 (m, 4H), 7.66-7.62 (m, 2H), 7.55-7.51 (m, 2H).

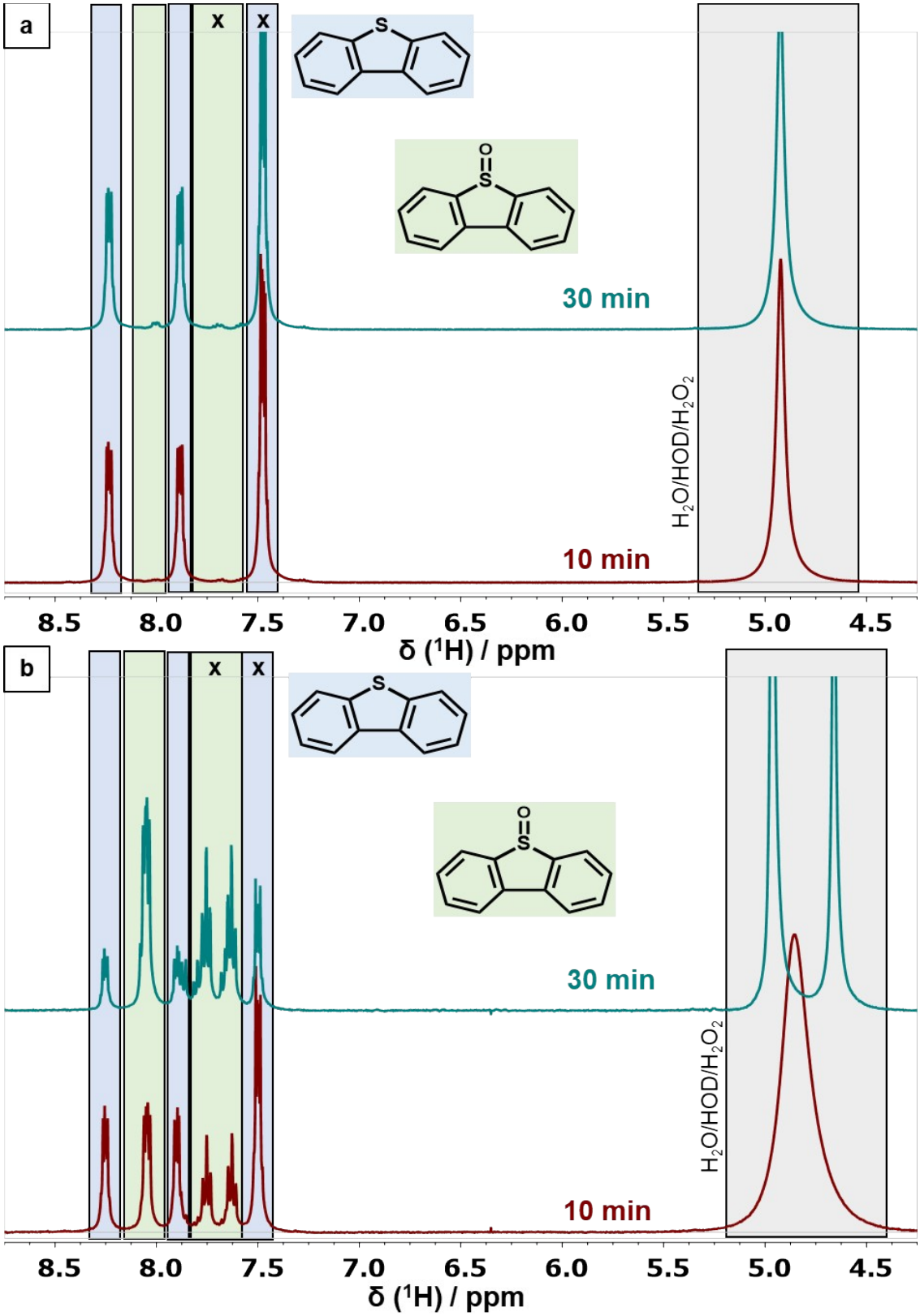

Fig. S20. (a) ^{1}H-NMR spectra of a standard catalysis (0.04 mmol dibenzothiophen, 0.06 mmol H_2O_2 (60 %), 0.85 mg WO_{3-x} nanorods in 0.6 mL of methanol-d_4) after 10 and 30 min. (b) ^{1}H-NMR spectra of an *ex situ* catalysis (0.04 mmol dibenzothiophen, 0.06 mmol H_2O_2 (60 %), 8.5 mg WO_{3-x} nanorods in 1 mL of methanol-d_4) after 10 and 30 min. **x** marking the peaks used for integration.

References

1 R. Dören, B. Leibauer, M. A. Lange, E. Schechtel, L. Prädel, M. Panthöfer, M. Mondeshki and W. Tremel, *Nanoscale*, 2021, **13**, 8146–8162.

2 O. S. Hammond, K. J. Edler, D. T. Bowron and L. Torrente-Murciano, *Nat. Commun.*, 2017, **8**, 14150.

3 E. Schechtel, R. Dören, H. Frerichs, M. Panthöfer, M. Mondeshki and W. Tremel, *Langmuir*, 2019, **35**, 12518–12531.

4 C.-T. Dinh, T.-D. Nguyen, F. Kleitz and T.-O. Do, *ACS Nano*, 2009, **3**, 3737–3743.

5 R. Ma, A.-H. Liu, C.-B. Huang, X.-D. Li and L.-N. He, *Green Chem.*, 2013, **15**, 1274.

6 B. Yu, C.-X. Guo, C.-L. Zhong, Z.-F. Diao and L.-N. He, *Tetrahedron Lett.*, 2014, **55**, 1818–1821.

7 E. P. Levanova, V. S. Nikonova, V. A. Grabel'nykh, N. V. Russavskaya, A. I. Albanov, I. B. Rozentsveig and N. A. Korchevin, *Russ. J. Gen. Chem.*, 2018, **88**, 383–388.

8 Spectral Database for Organic Compounds (SDBS), https://sdbs.db.aist.go.jp/sdbs/cgi-bin/direct_frame_top.cgi, (accessed 29 June 2021).

9 Y. Li, S. A.-E.-A. Rizvi, D. Hu, D. Sun, A. Gao, Y. Zhou, J. Li and X. Jiang, *Angew. Chem. Int. Ed.*, 2019, **58**, 13499–13506.

10 E. Voutyritsa, M. Garreau, M. G. Kokotou, I. Triandafillidi, J. Waser and C. G. Kokotos, *Chemistry*, 2020, **26**, 14453–14460.

11 B. Zhang, S. Li, S. Yue, M. Cokoja, M.-D. Zhou, S.-L. Zang and F. E. Kühn, *J. Organomet. Chem.*, 2013, **744**, 108–112.

12 L. Blank, M. Fagnoni, S. Protti and M. Rueping, *Synthesis*, 2019, **51**, 1243–1252.

13 C. Yang, Q. Jin, H. Zhang, J. Liao, J. Zhu, B. Yu and J. Deng, *Green Chem.*, 2009, **11**, 1401.

14 Y. Monguchi, T. Ida, T. Maejima, T. Yanase, Y. Sawama, Y. Sasai, S. Kondo and H. Sajiki, *Adv. Synth. Catal.*, 2014, **356**, 313–318.

15 D. Han, S. Li, S. Xia, M. Su and J. Jin, *Chemistry*, 2020, **26**, 12349–12354.

16 B. Yu, A.-H. Liu, L.-N. He, B. Li, Z.-F. Diao and Y.-N. Li, *Green Chem.*, 2012, **14**, 957.

17 B. Higginson, J. Sanjosé-Orduna, Y. Gu and R. Martin, *Synlett*, 2021.